Blackbody-radiation-induced resonances between Rydberg-Stark states of Na

E. J. Galvez, C. W. MacGregor,* B. Chaudhuri,† and S. Gupta
Department of Physics and Astronomy, Colgate University, Hamilton, New York 13346

E. Massoni‡ and F. De Zela
Departamento de Ciencias, Sección Física, Pontificia Universidad Católica del Perú, Lima, Peru

(Received 5 November 1996)

We report on measurements of the population of Rydberg states of Na in a constant electric field that result when 300-K blackbody radiation induces transitions from initial states with $|m|=0,1$ to neighboring states. Our measurements included comprehensive ranges of initial states ($n_i^*=24$–29), repopulation times ($t_d=0$–50 μs), and fields ($F_s=175$–712 V/cm). We find that the population is redistributed nonuniformly among states neighboring the initial state, reflective of sharp resonances between the states. By comparing calculations of transition probabilities in Na to the data for $F_s=200$ V/cm we were able to identify the populated states. Comparisons with calculations in H reveal that these resonances are hydrogenic. [S1050-2947(97)05704-1]

PACS number(s): 32.80.Rm, 32.70.Cs, 32.60.+i

I. INTRODUCTION

Spectroscopy of Rydberg states in electric fields has been one of the most important techniques to study the Stark effect. For fields below the saddle point, landmark spectroscopy experiments by Kleppner and co-workers [1] exposed the rich Stark structures of nonhydrogenic atoms and their striking departures from the hydrogen structure effected by the ionic core. For fields above the saddle point, structure was found for energies up to and above the zero-energy limit [2], revealing the physics of a regime where the applied field is as strong as the Coulomb field. More recently, ''scaled-energy'' spectroscopy experiments (i.e., tuning photon energy and field simultaneously) at medium-strength fields [3,4] have found structure that agrees remarkably well with calculations of the periodic orbits of the classical system, which exhibits core-induced chaos [4]. However, since the initial states of these and most other previous photoabsorption spectroscopy experiments were low-lying states, they tested the behavior of the Rydberg-Stark wave functions near the origin. For low fields the line intensities in the spectra can be explained by projecting of the Rydberg-Stark wave functions to zero-field angular momentum eigenstates if the initial state is well described in terms of the spherical basis (see, for example, Ref. [5]). An exception to this is the work in H [6,7], where the lower states were $n=10,11$ extremal parabolic Stark states. For high fields, above the saddle-point thresholds, the spectra have been explained in terms of oscillator strength densities [8]. Spectroscopic studies of nearby Rydberg-Rydberg transitions in electric fields, however, have not been possible because of the lack of broad-range far infrared sources. These latter studies could be an important testing ground for theoretical Stark-effect calculations [9].

In this article we report a type of experiment to study transitions between low-$|m|$ Rydberg-Stark states of Na in electric fields. The transitions included wavelengths from ~ 0.06 mm to ~ 1 mm. To our knowledge, this is the first type of experiment to cover such wide spectra in this wavelength range. In terms of the effective principal quantum number, defined as $n^*=1/\sqrt{-2E}$, where E is the energy given in atomic units (1 a.u.$=2.1946938\times 10^5$ cm^{-1} for Na), they corresponded to transitions from say $n_i^*\sim 26$ to $n_f^*=n_i^*+\Delta n^*$ for $|\Delta n^*|\sim 1-10$. We use a natural broadband source: 300-K blackbody radiation (BBR). This source is particularly useful because its spectrum is broad and well known. Spectroscopic plots of the data as a function of n^* were possible using the selective field ionization (SFI) detection technique. Two effects allowed us to lessen the standard limitations that SFI has when detecting field-free states. Large avoided crossings between low-$|m|$ Stark states in combination with low SFI slew rates prevented the states from acquiring significant energy shifts during SFI detection, and thus ionizing at or near their saddle-point fields. This allowed us, as will be shown below, to do Rydberg-Rydberg spectroscopy using SFI.

II. EXPERIMENTAL METHOD

Our experimental setup has been described in detail earlier [10]. Briefly, we excite Na atoms in an effusive atomic beam in the presence of a static electric field F_s to Rydberg states in the range $n=24$–29. The field F_s was above the value where adjacent Stark manifolds with $n>24$ merge. The excitation was done in two steps using 5-ns-long (full width at half maximum) π-polarized laser pulses, via the $3p_{3/2}$ intermediate state. The atoms were excited to $m=0$ and $|m|=1$ Stark states because of fine structure mixing of these m sublevels in the intermediate state. The bandwidth of the laser light was of about 10 GHz. For the case discussed in detail below, where $F_s=200$ V/cm, Na atoms were excited to individual same $|m|$ states near the middle of the manifolds (n_i^* is an integer) and two or three same $|m|$ states

*Present address: Department of Physics and Astronomy, University of Wyoming, Laramie, WY 82071.

†Present address: Department of Physics, Cornell University, Ithaca, NY 14853.

‡Present address: Facultad de Física, Pontificia Universidad Católica de Chile, Santiago, Chile.

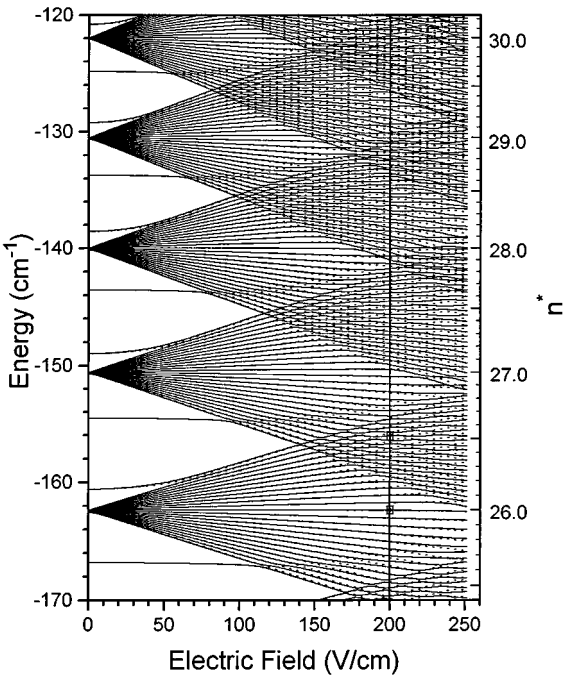

FIG. 1. Stark map of $m=0$ states (solid lines) and $|m|=1$ states (dotted lines) of Na in the region where we performed the experiments at $F_s=200$ V/cm. The two full circles mark the initial states for the two cases discussed in the text. The boxes surrounding the circles have a horizontal dimension representing the uncertainty in the field, and a vertical dimension representing the laser linewidth.

where the manifolds merge (n_i^* is a half integer). This can be seen in the energy-level structure of Na of Fig. 1.

Once the atoms were excited, blackbody radiation from the environment in the vacuum chamber (i.e., with a temperature $T=300$ K) induced transitions between the states. While continuous, the BBR energy density dropped significantly for the range of transitions with $|\Delta n^*|<1$, making our results not very sensitive to them. It was not worthwhile doing more elaborate experiments at greater temperatures since the BBR energy density at the corresponding frequencies modestly increased with T.

A time t_d after excitation the atoms were detected using selective field ionization, with a low-slew-rate [~ 200 V/(cm μs)] linearly rising electric field F_i, which varied from F_s to $F_h \sim 1000$ V/cm. We detected the electrons from the ionized atoms with an electron detector-multiplier, which consisted of two stacked microchannel plates and a 50-Ω impedance matched anode. Secondary electron emission [11] from the lower plate of the detector was not an important effect for the range of n studied here. The signals were recorded with a 500-MHz digital oscilloscope (HP model 54522) with an effective vertical resolution of 10 bits. Typical scans were an average of 256 single-shot traces of the oscilloscope.

The field ionization of the states proceeded through adiabatic paths for our slew rates. As mentioned earlier, since the detected states did not experience significant energy shifts as the ionizing field increased, the ''center'' of the ionization signal appeared at times $t_{\rm SFI} \propto F_i \propto (n^*)^{-4}$, measured from the beginning of the rise of the field. This enabled us to plot our data as a function of the value of n^* of the populated state, and thus obtain a direct measurement of the populations of the states. This is in contrast to the case of field free states, where large and different energy shifts produced by the ionizing field preclude an unambiguous transformation of the temporal scale of the signals to one in terms of n^* ($=n-\delta$, where δ is the quantum defect).

We transformed the experimental (temporal) scale to n^* using the relation $n^*=(At_{\rm SFI}^2+Bt_{\rm SFI}+C)^{-1/4}/2$, where A, B, and C where obtained from a fit to a set of measurements of $t_{\rm SFI}(n^*)$ for $n^*=24,24.5,\ldots,35$. This amounted to assuming a nearly linear relation between $t_{\rm SFI}(n^*)$ and $F(n^*)=1/[16(n^*)^4]$. Put in terms of n^*, the residuals of the fit had a standard deviation of 0.09. In addition, the signal from any state exhibited in general more than one peak, an effect that is caused by the dynamics of the ionization process [12–14], and one that ultimately limits the resolution of low-slew-rate SFI. In terms of n^*, the average width of the signal of the excited states was measured to be 0.31 with a standard deviation of 0.06. We used the center of each structure for the value of $t_{\rm SFI}(n^*)$. With this method we were therefore able to distinguish *unambiguously* between the signals of Stark states that were separated by $|\Delta n^*|>0.4$. This is the best resolution obtained with SFI for such a wide and continuous range of $|m|=0,1$ states.

III. RESULTS AND DISCUSSION

We have performed measurements of the population transfers between adjacent Rydberg states for the following parameter ranges: $n_i=24-29$, $t_d=0-50$ μs, and $F_s=175-712$ V/cm. The generic behavior was that as t_d was increased BBR induced transitions to a number of states that was small compared to the total number of channels available. When comparing the spectra for different initial states n_i and n_i', with $|n_i-n_i'|\sim p$, we found similarities when p is an integer, and substantial (and largest) differences when p is a half integer. The resonance-rich character of the spectra did not change as F_s was varied from fields where adjacent manifolds merged to fields just below the ionization thresholds of the initial states.

Here we show data taken at $F_s=200$ V/cm for two distinct cases that are representative of the larger data set that we took. They involve the cases where the initial states were in regions with either minimal or maximal apparent state mixing. In order to compare these results with theoretical calculations we chose $t_d=30$ μs. This time represented a compromise between allowing BBR enough time to populate significantly a large number of states, and avoiding multistep population redistribution [10].

In Figs. 2 and 3 we show plots of the data and calculations for initial states in the ''purer'' ($n_i^*=26.00$) and ''mixed'' ($n_i^*=26.52$) regions of the Stark map of Fig. 1, respectively. The horizontal scale of Figs. 2 and 3 gives the value of n^* of the ($|m|=0$ or 1) state being detected, obtained as discussed above. The signals of states with $|m|\geq 2$, populated by BBR-induced transitions, could not be resolved because atoms in those states followed partial or fully diabatic routes towards ionization with our slew rates. Previous studies [15] have shown that such signals contribute to a broad background. We believe that most of the background seen in Figs. 2 and 3 is caused by the unresolved signals of the $|m|=2$ states. Accurate modeling of the popu-

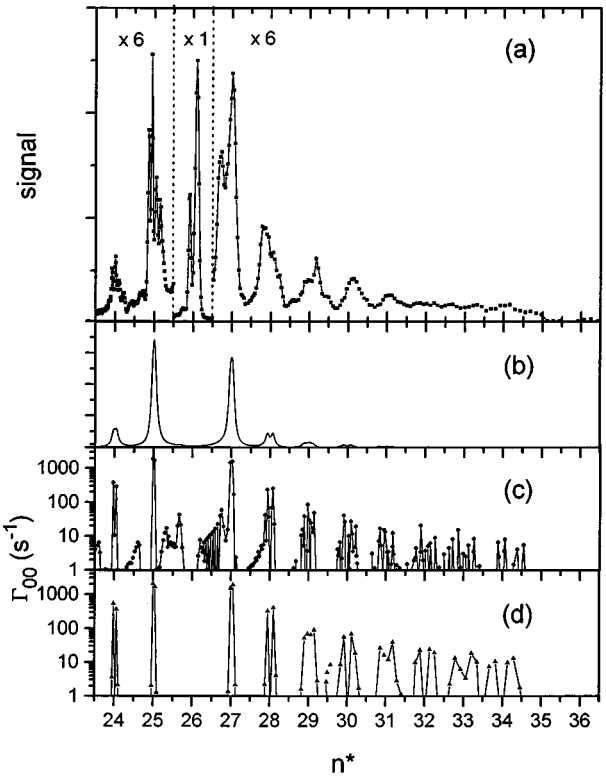

FIG. 2. (a) Experimental data for the case $n_i^* = 26.00$ at 200 V/cm, and $t_d = 30$ μs; (b) total transition probabilities Γ_T (see text) from the initial states to all final states convoluted with an experimental width (for Na); (c) transition probabilities Γ_{00} in Na; (d) transition probabilities Γ_{00} in H when the initial state is [26,13,12,0].

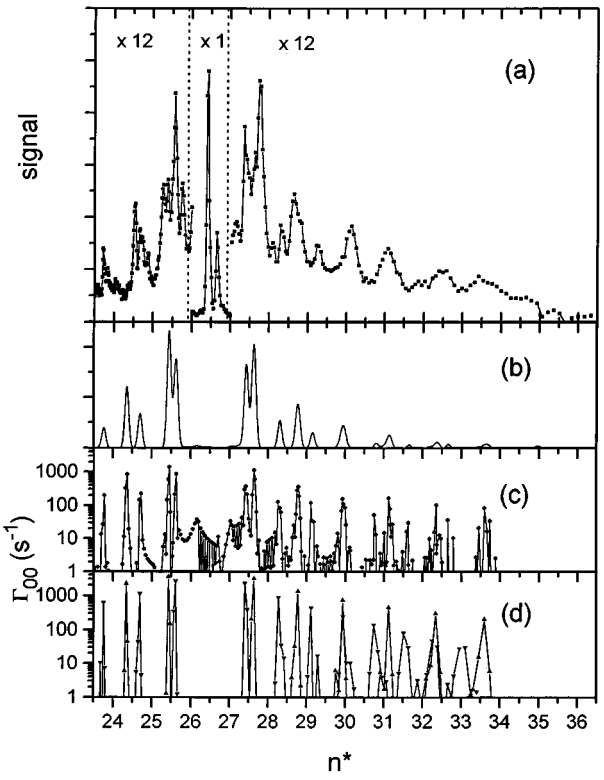

FIG. 3. (a) Experimental data for the case $n_i^* = 26.52$ at 200 V/cm, and $t_d = 30$ μs; (b) total transition probabilities Γ_T (see text) from the initial states to all final states convoluted with an experimental width (for Na); (c) transition probabilities Γ_{00} in Na; (d) transition probabilities Γ_{00} in H for the case where the initial states are [26,22,3,0] (triangles) and [27,5,21,0] (inverted triangles).

lations of these states is very difficult and hard to check.

Concentrating on the data of Figs. 2(a) and 3(a), we see that the largest signal comes from the initial states, with $n_i^* = 26.00, 26.52$, respectively. Adjacent to the initial states are well defined and reproducible peaks representing the population of (mostly upper) neighboring states populated by BBR-induced transitions. The signal drops for $n^* \sim 35$ due to ionization by the static field F_s. We did not see any evidence of collisional transfers: the data did not change when we lowered the atomic beam density by as much as an order of magnitude.

In the limit where the lifetimes of the initial and final states are the same, and for times short enough that multistep transitions are negligible, the growth of the signal of a final state is proportional to the transition probability from the initial state. In an effort to understand the data we have done calculations of the BBR-induced transition probabilities from the initial states to all final states aimed at identifying the states that produce the experimental signal. These calculations consisted of calculating the matrix elements between all the eigenstates, and computing the spontaneous and induced transition probabilities (using the 300-K BBR distribution). The calculations followed a numerical solution of the Stark problem using the method of Ref. [1] for $F_s = 200$ V/cm, using the basis of states from $n = 21$ to $n = 34$, for both $m = 0$ and $|m| = 1$ cases. While these calculations do not fully explain the populations, as discussed below, they serve to identify the states that would be populated by one-step transitions from the initial state.

In Figs. 2(b) and 3(b) we show an approximate modeling of the experimental data consisting of the sum of the transition probabilities

$$\Gamma_T(n^*) = 2[\Gamma_{00}(n^*) + \Gamma_{01}(n^*)]/3 + [\Gamma_{10}(n^*) + \Gamma_{11}(n^*)]/3, \quad (1)$$

where $\Gamma_{ij}(n^*)$ is the total transition probability (spontaneous plus BBR induced) from state $|m| = i$ to the state with $|m| = j$ at n^*, convoluted with an empirically determined experimental width. The weight of the probabilities are the squares of the Clebsch-Gordan coefficients corresponding to the expansion of the $3p_{3/2}(m_j = 1/2)$ state in terms of the m_ℓ substates (denoted here by ''m'') [16]. This assumes that the $m = 0$ and $|m| = 1$ states are degenerate within the bandwidth of the laser beam. Within the resolution of SFI we see good agreement in the positions of the peaks in the data and calculations. This is especially true for the case of Fig. 3, where the population is redistributed to a larger number of states than for the case of Fig. 2, as discussed below. In Figs. 2(c) and 3(c) we show the results of individual calculations for the $m = 0 \rightarrow m = 0$ case.

We can understand the main features of the distribution of transition probabilities in terms of hydrogenic transition-matrix elements. It is well known that hydrogen matrix elements between Stark states are non-negligible when the parabolic quantum numbers (n_1 or n_2) change by an amount that

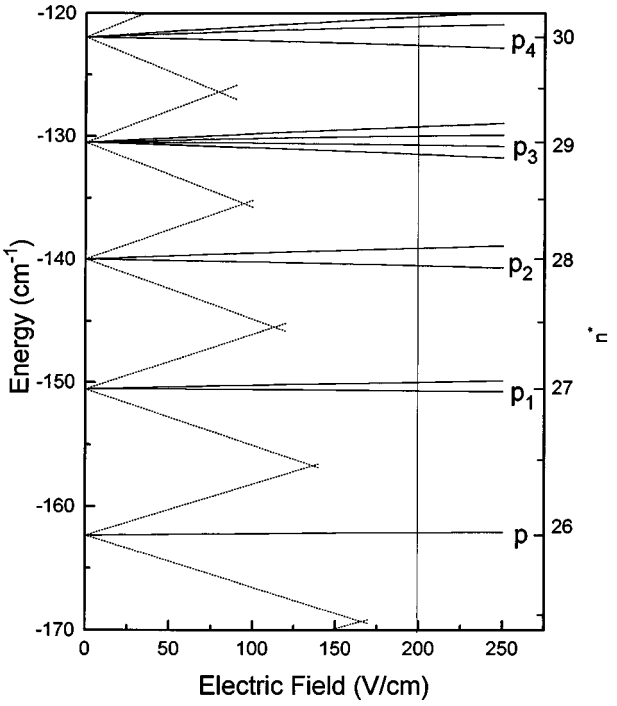

FIG. 4. Simplified energy level structure in H, showing the initial state $p=[26,13,12,0]$ at 200 V/cm, and neighboring states p_i's to which Γ_{00} are the highest.

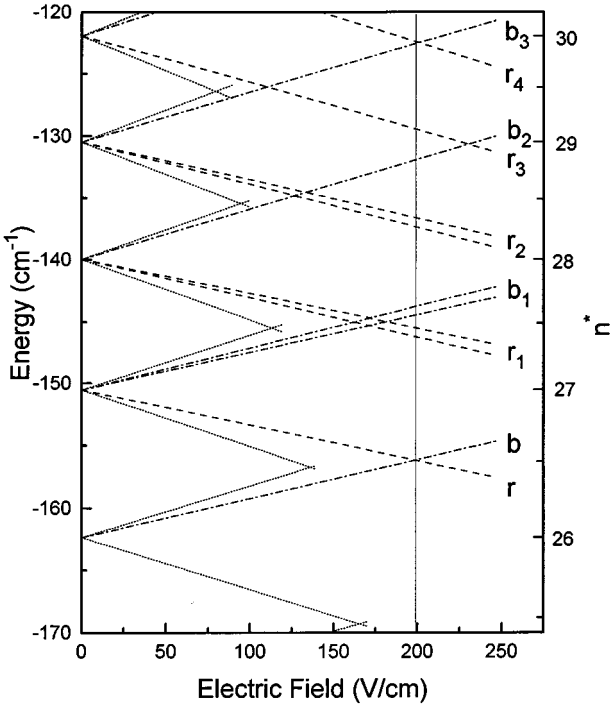

FIG. 5. Simplified energy level structure in H, showing the initial hydrogenic states: $b=[26,22,3,0]$ (blue) and $r=[27,5,21,0]$ (red) that have $n^*\sim 26.52$ at 200 V/cm, and the states to which the probabilities are the highest: b_i's for the blue case (dash-dotted lines), and r_i's for the red case (dashed lines).

is nearly the change in the principal quantum number for the transition (e.g., $[n,n_1,n_2,m]\rightarrow[n\pm p,n_1\pm p,n_2,m]$ if $n_1\gg n_2$ and $\rightarrow[n\pm p,n_1,n_2\pm p,m]$ if $n_1\ll n_2$) [7,17,18]. An alternative way to put it is that matrix elements will be largest between states with similar values of $(n_1-n_2)/n$. This propensity rule can be understood qualitatively by analyzing the spatial probability distribution of the hydrogenic wave functions; the states with low values of say n_1 have probability distributions concentrated at one side of the nucleus while the converse is true for high values of n_1. Therefore, only wave functions with significant spatial overlap will have non-negligible matrix elements.

For the case of Fig. 2, the initial state can be roughly associated with the [26,13,12,0] parabolic hydrogenic state, labeled as p in Fig. 4. Transition probabilities from p are highest to states $p_1=$([27,13,13,0], [27,14,12,0]), $p_2=$([28,13,14,0], [28,15,12,0]), $p_3=$([29,13,15,0], [29,14,14,0], [29,15,13,0], [29,16,12,0]), and $p_4=$([30,14,15,0], [30,16,13,0], [30,17,12,0]), shown (in order of ascending energy) in Fig. 4. These states are the maxima in Fig. 2(d). In addition, the positions of the hydrogenic probabilities in Fig. 2(d) were taken from the value of n^* that they have at 200 V/cm. We can see remarkable similarities between the calculated probabilities of Na and H.

The signals and calculations of Fig. 3 reveal much more complexity than those of Fig. 2. However, in similar ways, the data and calculations agree well, and all the peaks can be understood in terms of hydrogenic transitions. The most important features of Fig. 3 are the two peaks at $n^*\sim 27.4$ and 27.7, the three peaks at $n^*\sim 28.3$, 28.8, and 29.2, and the single peak at $n\sim 30$. In this case the initial state, at $n^*=26.52$, can be approximated by a mixture of the ''blue'' (upper going) [26,22,3,0] hydrogenic state (labeled ''b'' in Fig. 5), and the ''red'' (lower going) [27,5,21,0] hydrogenic state (labeled ''r'' in Fig. 5). The largest transition probabilities from state b are to states $b_1=$([27,22,4,0], [27,23,3,0]), $b_2=$ [28,25,2,0] and $b_3=$ [29,25,3,0] [triangles in Fig. 3(d) and dash-dotted lines in Fig. 5]. Similarly, state $r=[27,5,21,0]$ has large transition probabilities to states $r_1=$([28,5,22,0], [28,6,21,0]), $r_2=$([29,5,23,0], [29,6,22,0]), $r_3=$ [30,5,24,0], and $r_4=$ [31,5,25,0] [inverted triangles in Fig. 3(d) and dashed lines in Fig. 5]. Referring to Fig. 5, it can be seen that while states b and r have the same energy, with $n^*\sim 26.5$ at 200 V/cm, the red and blue states in the next higher manifold to which transitions occur do not have the same energies at 200 V/cm [i.e., $n^*(r_1)\sim 27.4$ and $n^*(b_1)\sim 27.7$], producing the two observed peaks. Similarly, the red and blue states two manifolds above are even more separated in energy at 200 V/cm [$n^*(r_2)\sim 28.3$ and $n^*(b_2)\sim 28.8$]. Since the Stark manifolds overlap more for higher n, the red state of the $n=30$ manifold, r_3, is near the above-mentioned states, at $n^*(r_3)\sim 29.1$. Therefore the three peaks correspond to the signal of states r_2, b_2, and r_3. Finally, r_4 and b_3 have an accidental degeneracy at 200 V/cm, producing the peak at $n^*\sim 30$. Similarly to the previous case, the qualitative agreement in the $m=0\rightarrow m=0$ probabilities for Na and H is good.

A more accurate modeling of the $m=0,1$ populations involves accounting for multistep transitions and radiative decay, which is done by solving the corresponding set of coupled rate equations [10]. The most challenging aspect of this is the calculation of radiative lifetimes for all the states involved. The challenge though is not so much theoretical but computational. Clearly, the method of Ref. [1] is very

cumbersome and inefficient for this type of calculation, and new more direct ways to calculate the wave functions need to be developed.

IV. CONCLUSIONS

In summary, we report of a type of experiment to study Rydberg-Rydberg transitions in the presence of an electric field. Our results, which show abundant structure, are explained qualitatively by calculations in Na, but more strikingly, by calculations in H. This suggests that the Stark wave functions in Na are very similar to those in H. Taking this into consideration may enable easy production of new types of Rydberg wave packets by exciting suitable initial Rydberg-Stark states of Na with terahertz pulses [19]. While these results are not of the quality of conventional spectroscopy, they are excellent in terms of SFI being used as a spectroscopic tool in this difficult-to-access spectral regime. Experiments with higher spectroscopic resolution will have to use more elaborate detection methods. One such method could consist of ''dumping'' the population of individual Stark states, via stimulated emission using a tunable laser, to a lower state such as $4s$, and detecting either the latter state's fluorescence cascades or the loss of SFI signal. Finally, it will be interesting to investigate if these types of transitions in heavier alkali-metal atoms, where core effects are more important, can also be explained in terms of hydrogenic transitions.

ACKNOWLEDGMENTS

We thank T. Bergeman, H. Castillo, M. Mehta, and L. Moorman for their help and useful discussions. We also thank the International Centre for Theoretical Physics of Trieste for travel support. This work was supported by Colgate University and NSF-RUI Grant No. PHY-9123702.

[1] M.G. Littman, M.L. Zimmerman, T.W. Ducas, R.R. Freeman, and D. Kleppner, Phys. Rev. Lett. **36**, 788 (1976); M.L. Zimmerman, M.G. Littman, M.M. Kash, and D. Kleppner, Phys. Rev. A **20**, 2251 (1979).

[2] R.R. Freeman, N.P. Economou, G.C. Bjorklund, and K.T. Lu, Phys. Rev. Lett. **41**, 1463 (1978); R.R. Freeman and N.P. Economou, Phys. Rev. A **20**, 2356 (1979).

[3] U. Eichmann, K. Richter, D. Wintgen, and W. Sandner, Phys. Rev. Lett. **61**, 2438 (1988).

[4] M. Courtney, H. Jiao, N. Spellmeyer, and D. Kleppner, Phys Rev. Lett. **73**, 1340 (1994); M. Courtney, H. Jiao, N. Spellmeyer, D. Kleppner, J. Gao, and J.B. Delos, *ibid.* **74**, 1538 (1995); M. Courtney, N. Spellmeyer, H. Jiao, and D. Kleppner, Phys. Rev. A **51**, 3604 (1995).

[5] T.F. Gallagher, *Rydberg Atoms* (Cambridge University Press, London, 1994).

[6] P.M. Koch, in *Rydberg States of Atoms and Molecules*, edited by R.F. Stebbings and F.B. Dunning (Cambridge University Press, London, 1983).

[7] M. Bellermann, T. Bergeman, A. Haffmans, P.M. Koch, and L. Sirko, Phys. Rev. A **46**, 5836 (1992).

[8] D.A. Harmin, Phys. Rev. Lett. **49**, 128 (1982); Phys. Rev. A **26**, 2656 (1982).

[9] G.D. Stevens, C.-H. Iu, T. Bergeman, H.J. Metcalf, I. Seipp, K.T. Taylor, and D. Delande, Phys. Rev. A **53**, 1349 (1996).

[10] E.J. Galvez, J.R. Lewis, B. Chaudhuri, J.J. Rasweiler, H. Latvakoski, F. De Zela, E. Massoni, and H. Castillo, Phys. Rev. A **51**, 4010 (1995).

[11] S. Gupta and E.J. Galvez (unpublished).

[12] P.M. Koch and D. Mariani, Phys. Rev. Lett. **46**, 1275 (1981).

[13] J.-L. Vialle and H.T. Duong, J. Phys. B **12**, 1407 (1979).

[14] G.B. McMillian, T.H. Jeys, K.A. Smith, F.B. Dunning, and R.F. Stebbings, J. Phys. B **15**, 2131 (1982); W. van de Water, D. Mariani, and P.M. Koch, Phys. Rev. A **30**, 2399 (1984).

[15] T.H. Jeys, G.W. Foltz, K.A. Smith, E.J. Beiting, F.G. Kellert, F.B. Dunning, and R.F. Stebbings, Phys. Rev. Lett. **44**, 390 (1980); T.H. Jeys, G.B. McMillian, K.A. Smith, F.B. Dunning, and R.F. Stebbings, Phys. Rev. A **26**, 335 (1982).

[16] T.H. Jeys, G.B. McMillian, K.A. Smith, F.B. Dunning, and R.F. Stebbings, Phys. Rev. A **26**, 335 (1982).

[17] H.A. Bethe and E.E. Salpeter, in *Quantum Mechanics of One- and Two-Electron Atoms* (Springer, Berlin, 1957); Phys. Rev. A **46**, 5836 (1992).

[18] Several groups have exploited this effect in H for studying field ionization of Stark states [cf. P.M. Koch and D. Mariani, Phys. Rev. Lett. **46**, 1275 (1981)] and multiphoton ionization of one-dimensional states [cf. J.E. Bayfield and L.A. Pinnaduwage, Phys. Rev. Lett. **54**, 313 (1985)].

[19] L. Xu, X.-C. Zhang, and D.H. Auston, Appl. Phys. Lett. **61**, 1784 (1992), and references therein.